Supporting Information

Two-dimensional Blue-AsP Monolayers with Tunable Direct Band Gap and Ultrahigh Carrier Mobility Show Promising High-performance Photovoltaic Properties

Xinyong Cai,[a, 1] Yuanzheng Chen,[a, 1, *] Bai Sun,[a, e] Jiao Chen,[a] Hongyan Wang,[a] Yuxiang Ni,[a] Li Tao,[b] Hui Wang,[a, c] Shouhui Zhu,[a] Xiumei Li,[a] Yanchao Wang,[c] Jian Lv,[c] Xiaolei Feng,[f] Simon A.T. Redfern,[f] and Zhongfang Chen[d, *]

[a] *School of Physical Science and Technology, Key Laboratory of Advanced Technologies of Materials, Ministry of Education of China, Southwest Jiaotong University, Chengdu 610031, China.*

[b] *School of Optoelectronic Technology, Chengdu University of Information Technology, Chengdu 610225, China*

[c] *State Key Lab of Superhard Materials, College of Physics, Jilin University, Changchun 130012, China*

[d] *Department of Chemistry, University of Puerto Rico, Rio Piedras Campus, San Juan, PR 00931, USA*

[e] *Department of Mechanics and Mechatronics Engineering, Centre for Advanced Materials Joining, Waterloo Institute of Nanotechnology, and Department of Physics and Astronomy, University of Waterloo, Waterloo, Ontario N2L 3G1, Canada*

[f] *Department of Earth Sciences, University of Cambridge, Cambridge, CB2 3EQ, UK*

[1] *These authors contributed equally*

E-mail: cyz@calypso.org.cn or zhongfangchen@gmail.com

Details of structure prediction

The particle swarm optimization (PSO) method within the evolutionary algorithm as implemented in the CALYPSO code[1,2] was employed to find the lowest energy structures of As_xP_{1-x} monolayer (x = 3/4, 2/3, 3/5, 1/2, 2/5, 1/3, and 1/4). Unit cells containing 1, 2, 3, and 4 formula units (f.u.) were considered. In the first step, random structures with certain symmetry are constructed in which atomic coordinates are generated by the crystallographic symmetry operations. Local optimizations using the VASP code[3] were done with the conjugate gradients method and terminated when the Gibbs free energy converged with changes smaller than 1×10^{-5} eV per cell. After processing the first-generation structures, 60% of them with lower Gibbs free energies were selected to construct the next generation structures by PSO. 40% of the structures in the new generation were randomly generated. A structure fingerprinting technique with bond characterization matrix was applied to the generated structures, so that identical structures are strictly forbidden. These procedures significantly enhance the diversity of the structures, which is crucial for structural global search efficiency. In most cases, structural searching simulations for each calculation were stopped after generating 1000 ~ 1200 structures (e.g., about 20 ~ 35 generations).

Calculation methods for spectroscopic limited maximum efficiency (SLME):

The maximum solar cell efficiency is simulated through calculating spectroscopic limited maximum efficiency (SLME) based on the improved Shockley-Queisser model.[3] The SLME of a material takes into account the band gap size, the band gap type (direct versus indirect), and the optical absorption spectrum, all of which can be obtained from reliable first principles calculations. The calculation of radiative and non-radiative recombination current is based on detailed balance theory using the energy difference between the minimum band gap and direct-allowed gap as the input. The simulation is performed under the standard AM1.5G solar spectrum at room temperature.

The related data of discussions in the paper:

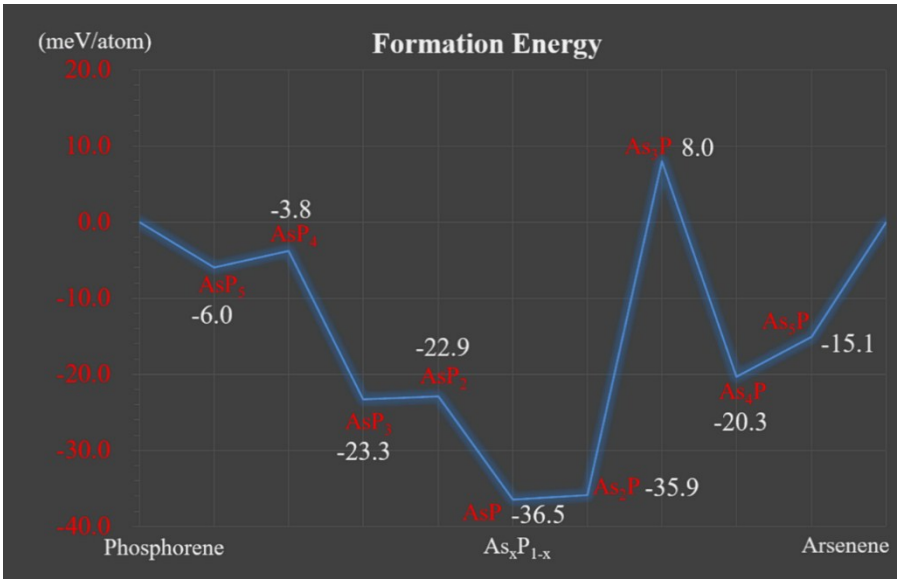

Figure S1. The convex hull for the formation energies ($\Delta\varepsilon$)of 2D As_xP_{1-x} monolayers by the following expression: $\Delta\varepsilon_{As_xP_{1-x}} = \varepsilon_{As_xP_{1-x}} - x\varepsilon_{As} - (1-x)\varepsilon_P$, where $\varepsilon_{As_xP_{1-x}}$, ε_{As} and ε_P are the energies of 2D As_xP_{1-x} monolayers, gray arsenene, and black phosphorene, respectively.

Table S1. The optimized structural parameters of monolayer x-AsP (x= I, II, III, IV, V) polymorphs.

Structure	Space Group	Lattice parameters	Element	Lattice parameters (x, y, z)		
I-AsP	*Cm*	a=5.96 b= 5.96 c= 21.43 α=91.6° β=91.6° γ= 119.8°	As1	0.1777	0.5199	0.4666
			As2	0.5199	0.1777	0.4666
			As3	0.1815	0.1815	0.5334
			P1	0.8562	0.5332	0.5284
			P2	0.5332	0.8562	0.5284
			P3	0.8353	0.8553	0.4719

Structure	Space Group	Lattice parameters	Element	Lattice parameters (x, y, z)		
II-AsP	*Cm*	a=3.45 b=11.94 c=21.44	As1	0.9623	0.0692	0.5339
			As2	0.4608	0.3210	0.5339
			As3	0.9336	0.8810	0.4661

		α= 97.2° β= 93.8° γ= 90.0°	As4	0.4616	0.8077	0.5339
			P1	0.4345	0.6279	0.4706
			P2	0.9576	0.3884	0.4699
			P3	0.9344	0.3834	0.4699
			P4	0.4366	0.1389	0.4720

Structure	**Space Group**	**Lattice parameters**	**Element**	**Lattice parameters (x, y, z)**		
III-AsP	*Cm*	a=9.13 b=9.13 c=21.52 α= 90.58° β= 90.58° γ= 21.70°	As1	0.3420	0.3420	0.9305
			As2	0.1162	0.1162	0.8607
			As3	0.6743	0.6743	0.9289
			P1	0.4516	0.4516	0.8678
			P2	0.0060	0.0060	0.9224
			P3	0.7856	0.7856	0.8689

Structure	**Space Group**	**Lattice parameters**	**Element**	**Lattice parameters (x, y, z)**		
VI-AsP	*P*-1	a=3.43 b=5.97 c=21.47 α= 97.9° β= 94.7° γ= 90.0°	As1	0.8558	0.8633	0.5347
			As2	0.3208	0.6021	0.4653
			P1	0.8239	0.1007	0.4715
			P2	0.3521	0.9672	0.5271

Structure	**Space Group**	**Lattice parameters**	**Element**	**Lattice parameters (x, y, z)**		
V-AsP	*P*-1	a=3.45 b=5.96 c=21.46 α= 88.1° β= 89.0° γ= 90.0°	As1	0.0045	0.6766	0.4660
			As2	0.9958	0.3234	0.5340
			P1	0.5026	0.1634	0.4724
			P2	0.4977	0.8366	0.5276

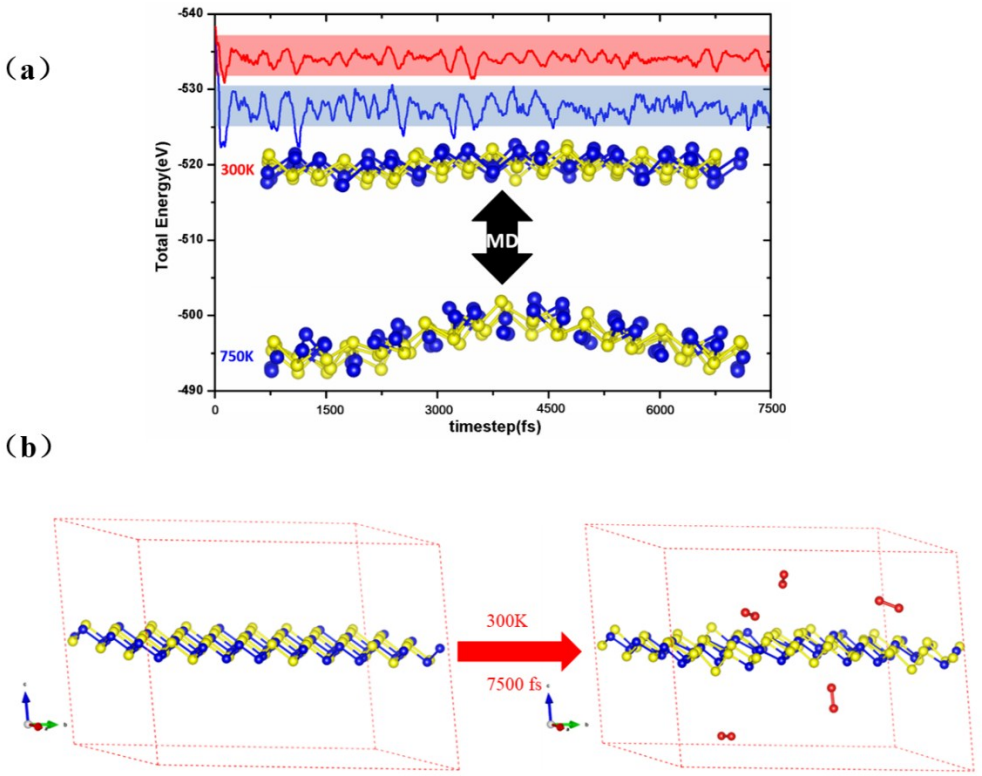

Figure S2. (a)The side views of snapshots and energy fluctuations of I-AsP at temperatures of 300 (red) and 750 K (blue) for 7.5 ps with a time step of 2 fs and one k-point. (b) AIMD simulations of I-AsP monolayer structure at 300 K in the O_2 atmosphere for 7.5 ps.

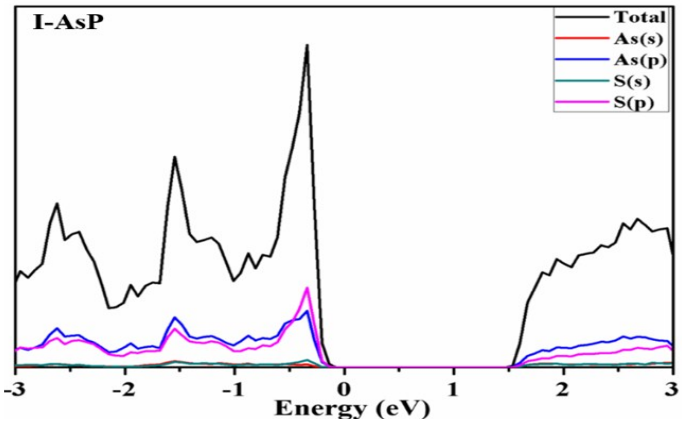

Figure S3. The density of states (DOS) of the I-AsP monolayer by PBE level

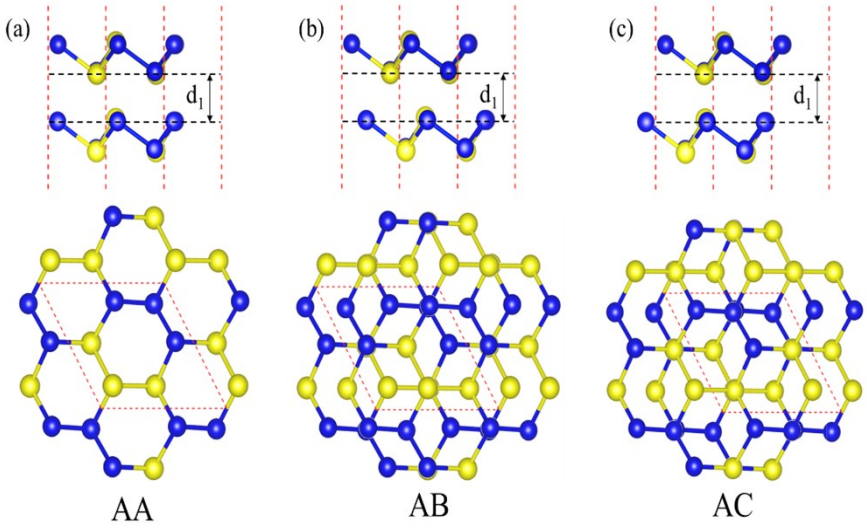

Figure S4. Side and top view of the different stacked layered structure of bilayer I-AsP.

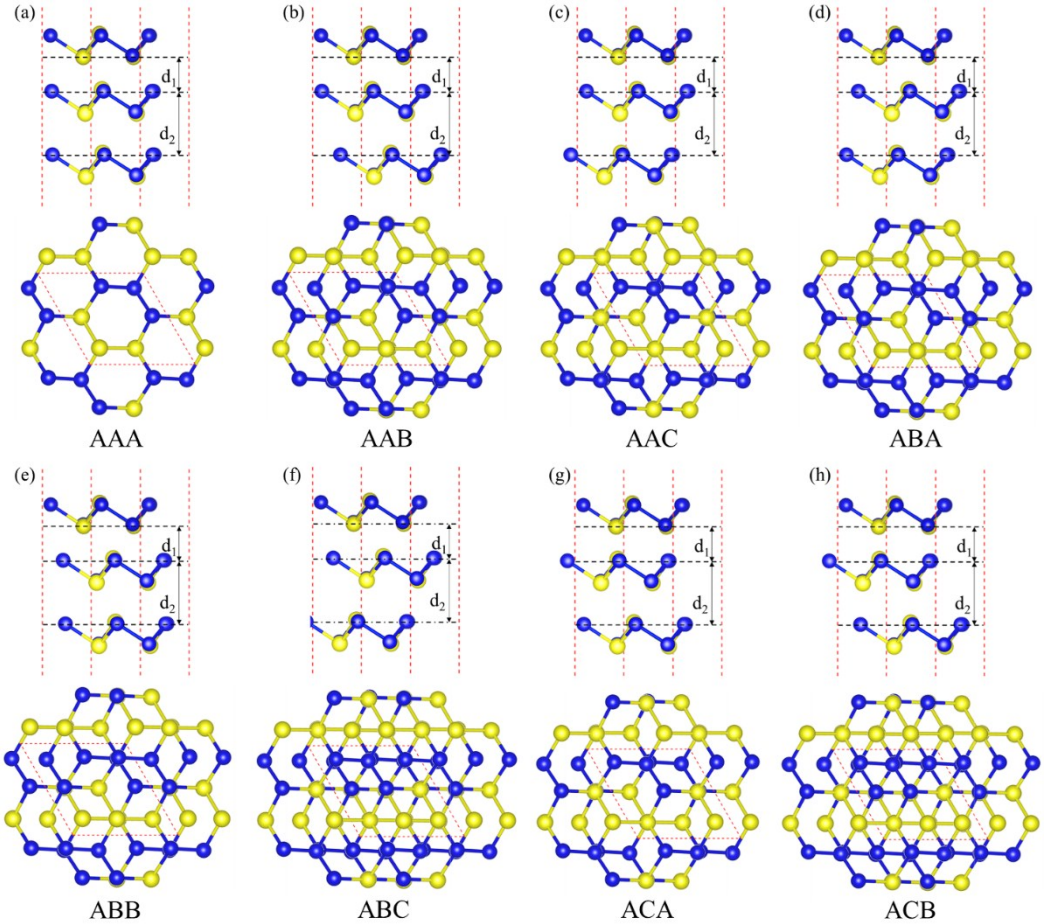

Figure S5. Side and top view of the different stacked layered structure of trilayer I-AsP.

Table S2. Calculated interlayer distances (d_1 and d_2), lattice parameter a, and cohesive-energy differences (∆E) based on different exchange-correlation levels for different stacking of bilayer I-AsP. Distances and lattice parameter are given in units of Å. ∆E are given in units of eV based on the ground state structure (AB stacking) calculated.

Stacking modes	**d_1**	**d_2**	**a**	**ΔE**
AA	3.19	-	5.92	0.02
AB	3.41	-	5.95	0.03
AC	3.22	-	6.02	0.02

Table S3. Calculated interlayer distances (d_1 and d_2), lattice parameter a, and cohesive-energy differences (∆E) based on different exchange-correlation levels for different stacking of trilayer I-AsP. Distances and lattice parameter are given in units of Å. ∆E are given in units of eV based on the ground state structure (ABC stacking) calculated.

Stacking modes	**d_1**	**d_2**	**a**	**ΔE**
AAA	2.85	2.85	5.92	0.03
AAB	2.85	3.04	5.94	0.02
AAC	2.84	2.98	6.02	0.02
ABA	3.02	3.04	5.94	0.02
ABB	3.04	2.85	5.94	0.04
ABC	2.71	2.71	5.96	0.00
ACA	3.02	3.30	5.98	0.03
ACB	2.98	3.25	5.9	0.03

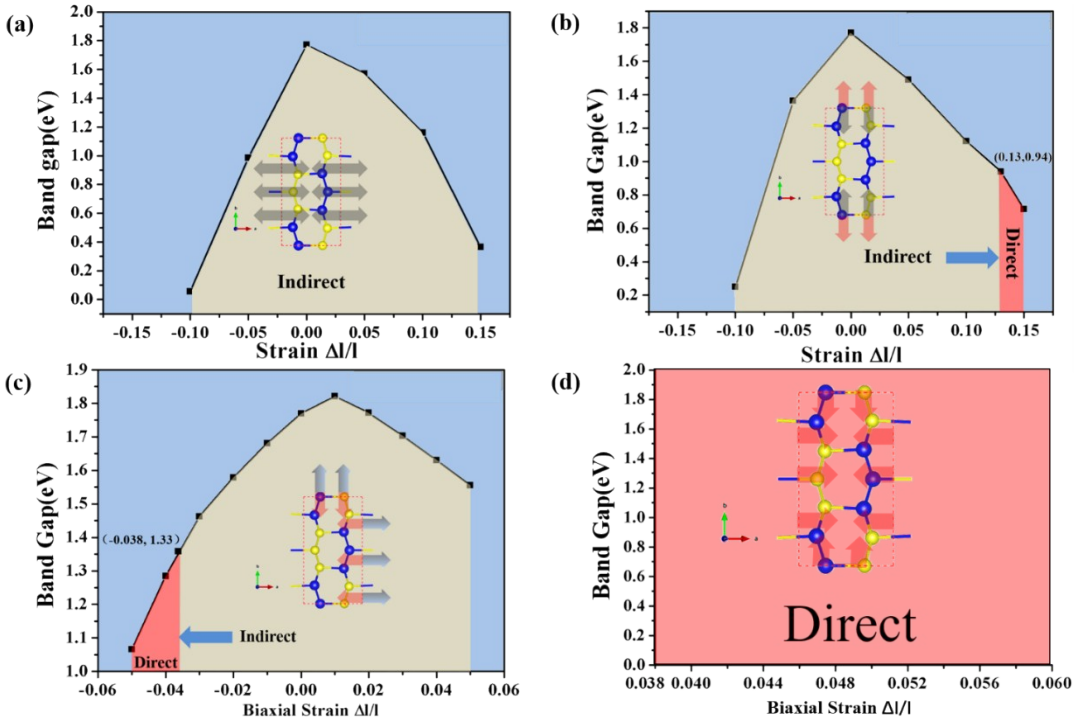

Figure S6. Dependence of the fundamental band gap on the in-plane stretching along (a) armchair direction, (b) zigzag direction, and (c) biaxial strain by PBE level. (d) The range of direct band gap on biaxial strain from 3.8% to 6% by HSE06 level

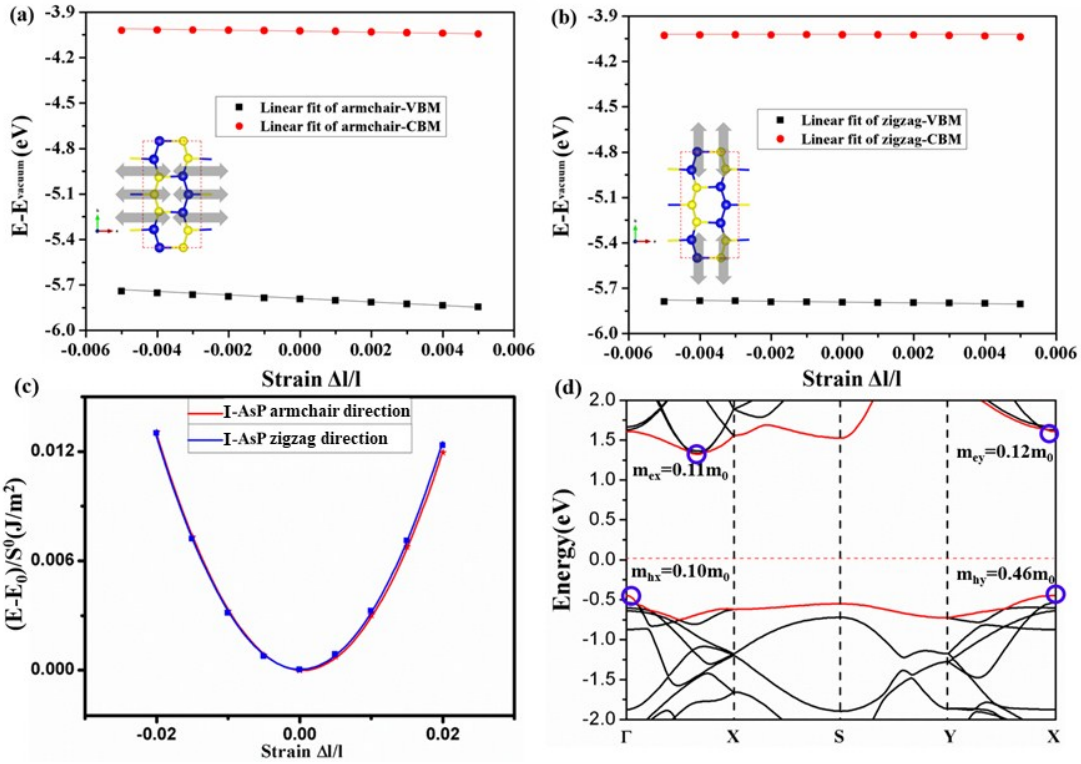

Figure S7. Relationship between energy shift of the band edge position and the dilation Δl/l along armchair (a) and zigzag (b) directions, respectively. (c) Total energy shift E-E_0 on per surface as a function of lattice deformation Δl/l along armchair and zigzag directions. (d) The effective masses of electronic (m_e) and hole (m_h) along Γ → X and Γ→ Y.

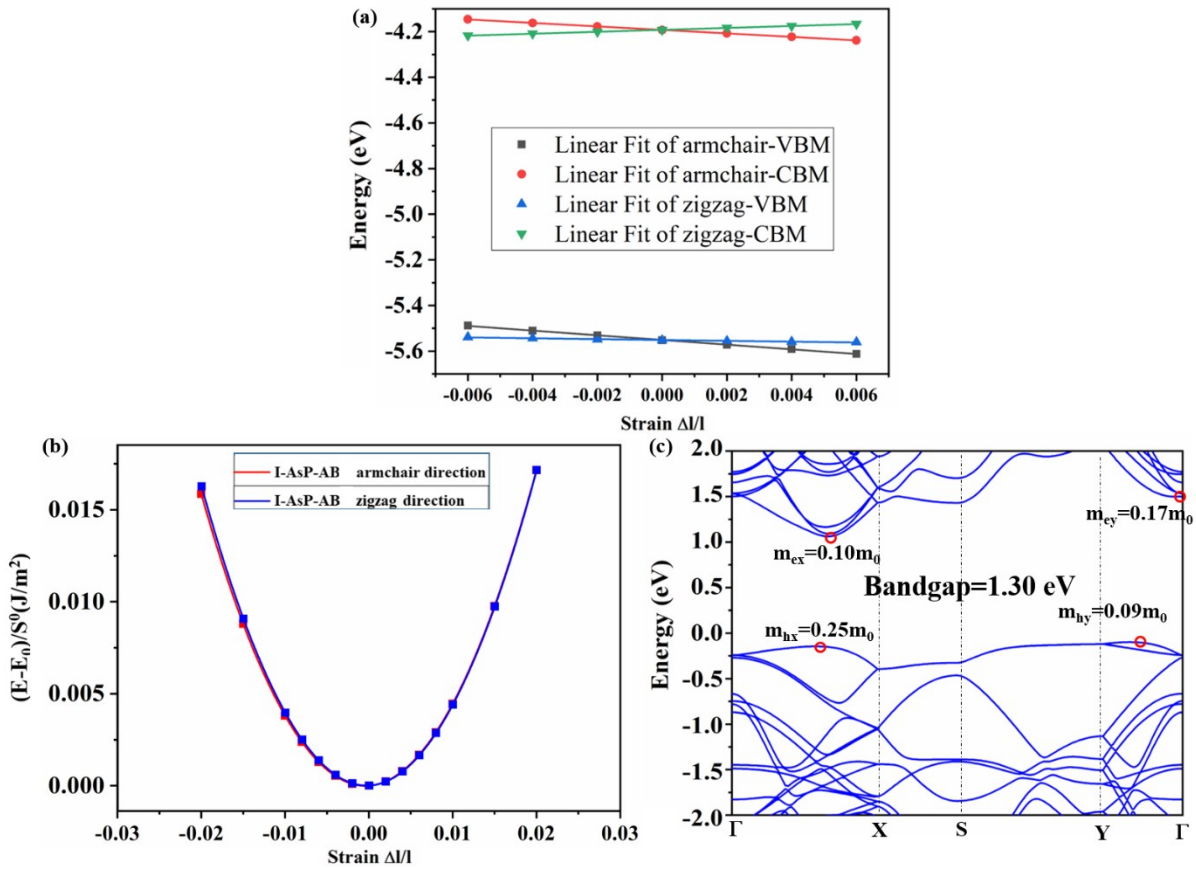

Figure S8. For the bilayer (AB) I-AsP. (a) Relationship between energy shift of the band edge position and the dilation **Δ**l/l along armchair and zigzag directions, respectively. (b) Total energy shift E-E_0 on per surface as a function of lattice deformation Δl/l along armchair and zigzag directions. (c) The effective masses of electronic (m_e) and hole (m_h) along Γ → X and Γ→ Y.

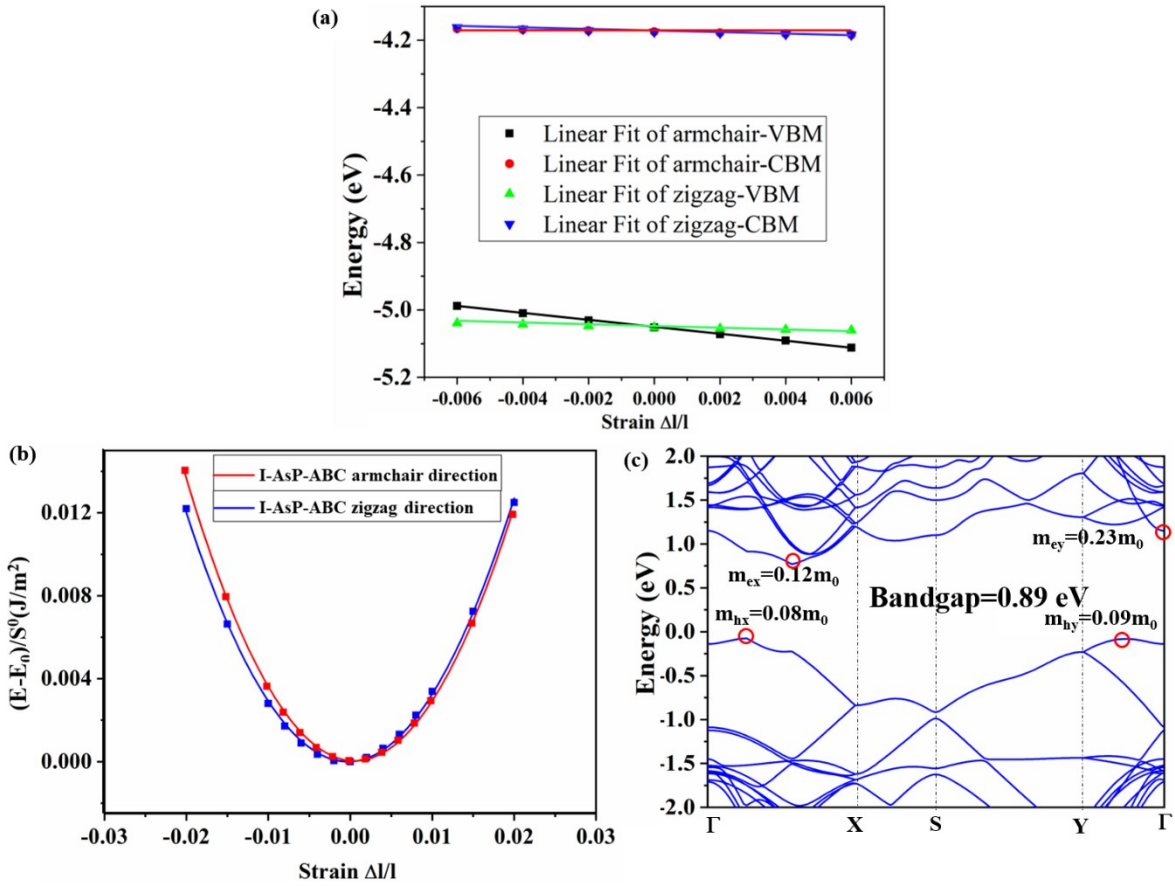

Figure S9. For the trilayer (ABC) I-AsP. (a) Relationship between energy shift of the band edge position and the dilation **Δ**l/l along armchair and zigzag directions, respectively. (b) Total energy shift E-E_0 on per surface as a function of lattice deformation Δl/l along armchair and zigzag directions. (c) The effective masses of electronic (m_e) and hole (m_h) along $\Gamma \rightarrow$ X and $\Gamma \rightarrow$ Y.

Table S4. Calculated effective mass (m^*/m_0), deformation potential constant (E_d), 2D elastic modulus C^{2D}, and mobility (μ) for electron (*e*) and holes (*h*) along zigzag (*y*) and armchair (*x*) directions for the bilayer (AB) and the trilayer (ABC) I-AsP.

	Direction		m^*/m_0	C^{2D} (Nm^{-1})	E_d (eV)	μ $cm^2V^{-1}s^{-1}$
bilayer	Armchair (*x*)	e	0.10	80.64	2.31	24.49× 10^3
		h	0.25	80.64	10.25	435
	Zigzag (*y*)	e	0.17	82.01	4.24	4.38× 10^3
		h	0.09	82.01	1.84	38.21× 10^3

trilayer	Armchair (*x*)	e	0.12	72.08	1.54	32.47×10^3
		h	0.08	72.08	10.26	2.15×10^3
	Zigzag (*y*)	e	0.23	74.14	1.84	12.21×10^3
		h	0.09	74.14	1.84	61.07×10^3

References

(1) Wang, Y.; Lv, J.; Zhu, L.; Ma, Y. CALYPSO: A Method for Crystal Structure Prediction. *Comput. Phys. Commun.* **2012**, 183, 2063–2070.

(2) Wang, Y.; Lv, J.; Zhu, L.; Ma, Y. Crystal Structure Prediction Via Particle-Swarm Optimization. *Phys. Rev. B*. **2010**, 82, 94116.

(3) Yu, L.; Zunger, A. *Phys. Rev. Lett.*, **2012**, 108, 068701.